Cross-linked chitosan/marble powder composites for the adsorption of Dimozol Blue

Deniz Akın Şahbaz and Caglayan Acikgoz

ABSTRACT

Cross-linked chitosan(C)/marble powder (M) composites with different weight ratio percentage (C100M0, C70M30, C50M50, and C30M70) were prepared from marble powder and chitosan and cross-linked using glutaraldehyde. The morphology and the surface area of the chitosan/marble powder composites were also characterized with a scanning electron microscope (SEM) and Micromeritics (ASAP 2020) BET (Brunauer, Emmett and Teller) instrument, respectively. To evaluate the adsorption behaviour of the chitosan/marble powder composites, 0.1 g adsorbent was added into 50 mL Diamozol Blue BRF %150 (C.I. Reactive Blue 221) solution with fixed concentrations (60 mg/L). At equilibrium, the adsorption capacity of C100M0, C70M30 and C50M50 for Dimozol Blue was about 27 mg/g and significantly greater than that of C30M70. C50M50 composite was more economical than C100M0 and C70M30 due to the higher marble powder content, and hence was selected as an adsorbent for the removal of Dimozol Blue from aqueous solution. The adsorption kinetics and equilibrium isotherms of Dimozol Blue onto the chitosan/marble powder composites from aqueous solution were investigated. The studies revealed that Dimozol Blue dye adsorption was described well by the pseudo-second-order and Freundlich isotherm models. The results of this study indicated the applicability of the chitosan/marble powder composites for removing industrial dyes from aqueous solution.

Key words | adsorption, chitosan, Dimozol Blue, marble powder

Deniz Akın Şahbaz
Chemical Engineering Department,
Afyon Kocatepe University,
Afyonkarahisar,
Turkey

Caglayan Acikgoz (corresponding author)
Chemical and Process Engineering Department,
Bilecik Şeyh Edebali University,
Bilecik,
Turkey
E-mail: *caglayan.acikgoz@bilecik.edu.tr*

INTRODUCTION

Several industries such as textile, food, cosmetic, pharmaceutical products, rubber, leather, and so on use dyes for their products. Industrial wastewater contaminated with dyes affects all living organisms in aquatic life because it has toxic and carcinogenic properties. Many techniques, such as filtration, oxidation, ozonation, adsorption, photocatalysis, and electrochemical treatment, have been employed to remove dyes from wastewater (Su *et al.* 2016). Among these techniques, adsorption stands out due to its low cost, easy operation, flexibility, and simplicity of design. Activated carbons are generally regarded as the most effective adsorbents used in adsorption processes due to their adsorptive properties and high surface areas (Yuliani *et al.* 2017). However, activated carbon has a high cost and difficulty in regeneration (Nesic *et al.* 2012). In the literature, relatively cheap alternative materials derived from industrial waste (Silva *et al.* 2016), agricultural waste (Singh *et al.* 2017), plant biomass (Bayramoglu *et al.* 2013), minerals (Dotto *et al.* 2016; Marrakchi *et al.* 2016; Arica *et al.* 2017), and resin (Bayramoglu *et al.* 2009; Yavuz *et al.* 2011) have been intensively investigated as alternatives for activated carbon.

Marble powder is a waste material produced in the millions of tons each year around the world. The wastes can cause three main problems: environmental pollution, environmental health issues, and economic loss (Alyamac *et al.* 2017). The reuse of waste marble powder as an adsorbent will provide an opportunity to obtain environmental and economic gains. However, unmodified marble powder shows less adsorption capacity for the removal of dye. A linear copolymer of glucosamine and *N*-acetyl glucosamine, chitosan is easily obtained by thermo-chemical deacetylation of crustacean chitin. Chitosan has excellent properties for adsorption of dyes due to the presence of amino (NH_2) and hydroxyl (OH) groups in the polymer matrix (Nesic *et al.* 2012). Moreover, natural abundance, biocompatibility, anti-bacterial properties, and biodegradability are other

doi: 10.2166/wst.2017.447

important characteristic features of chitosan, making it unique among other adsorbent materials (Khan *et al.* 2016). However, high cost, low chemical stability and dissolution in an acidic medium are drawbacks associated with the use of pure chitosan as an adsorbent. Immobilizing chitosan on a low-cost material is an effective modification method to provide enhanced mechanical, thermal or adsorption properties compared with any of its components used alone. Several studies have investigated the removal of dyes and metal ions from aqueous solution using chitosan-based composites such as chitosan/bentonite composite (Zhang *et al.* 2016), chitosan/clinoptilolite composite (Dinu & Dragan 2010) and chitosan/clay composite (Auta & Hameed 2014). However, it is observed that there is no report on the utilization of chitosan/marble powder composite as an adsorbent specifically for the removal of the dye molecules.

The objective of this study was to synthesize the chitosan/marble powder composites and analyze their adsorptive effectiveness in the removal of Dimozol Blue from aqueous solutions as potential low-cost, high performance adsorbents. The factors influencing the adsorption capacity of the composites, such as the contact time, pH value of dye solution, adsorbent dosage, initial concentration of dye solutions and temperature, were investigated. In order to examine the mechanism of the adsorption process, the kinetics, adsorption isotherms and thermodynamics were evaluated.

MATERIALS AND METHODS

Materials

The 75–85% deacetylated chitosan with a viscosity of 200–800 cP measured by Brookfield viscometer in 1% of chitosan solution in 1% acetic acid was purchased from Aldrich Chemical Corporation, Germany. The average molecular weight of chitosan is 190,000–310,000 Da. Aqueous acetic acid (Merck) solution was used as a solvent for the chitosan. Glutaraldehyde solution (Fluka, 50%) was used as a cross-linker. The marble powder was collected from the local marble cutting/processing industry in Bilecik, Turkey. The obtained marble powder was dried in an oven at 80 °C for 24 h and then passed through a sieve to obtain 90 μm size before use. Diamozol Blue BRF %150 (C.I. Reactive Blue 221) (purity of 99%) was obtained from a dye factory in Bursa, Turkey. The solubility of the dye is high in aqueous solution (100 g/L), even in the presence of alkali it has very good solubility. All chemicals were of analytical grade, and no further purification was required.

Preparation of chitosan/marble powder composites

To obtain a homogenous mixture, 2 g of chitosan was dissolved in 75 mL of 5% v/v acetic acid with constant stirring. The marble powder was added and the mixture was left overnight with continuous stirring on a magnetic stirrer. Then, the dispersion was taken in a syringe and allowed to fall slowly and dropwise into 500 mL of 1 M sodium hydroxide solution with gentle stirring, resulting in the formation of the chitosan/marble powder composites, which were kept in the same solution overnight with continuous stirring. To remove any residual sodium hydroxide, the wet chitosan/marble powder composites were washed many times with distilled water to attain a neutral pH. Subsequently, the composites were shaken in 2.5 w % glutaraldehyde ethyl alcohol solution for 15 h at 60 °C. In chitosan crosslinking with glutaraldehyde, the high process temperature (60 ± 1 °C) resulted in the formation of glutaraldehyde condensates that were also capable of covalent crosslinking and, additionally, could affect the enlargement of the surface of the composites (Jóźwiak *et al.* 2017). After the cross-linking reaction, the composites were washed using distilled water to remove free glutaraldehyde and then freeze-dried for 24–48 h. In this study, a series of chitosan/marble powder composites with different weight ratio percentages were synthesized, viz., 100:0 wt.% (henceforth denoted as C100M0), 70:30 wt.% (C70M30), 50:50 wt.% (C50M50), and 30:70 wt.% (C30M70).

Characterization of chitosan/marble powder composites

The surface morphology of the composites was observed with a scanning electron microscope (SEM, Bruker, Germany). To analyze the C, O, and Ca element content of the composites, elementary characterization was carried out using energy-dispersive spectroscopy (EDS, Bruker, Germany). Surface area of the chitosan/marble powder composites was measured by a Micromeritics (ASAP 2020) BET (Brunauer, Emmett and Teller) instrument using the nitrogen intrusion technique. The microstructure of the sorbent was characterized using physical adsorption/desorption of nitrogen at 77 K. Spectra of Fourier transform infrared spectroscopy (FTIR) for the bare chitosan and marble powder and chitosan/marble powder composites were obtained by a FTIR spectrophotometer (Agilent

Technologies, Cary 630 FTIR). The spectra were acquired in the wavenumber range from 4,000 to 400 cm^{-1}.

Adsorption studies

To evaluate the adsorption behaviour of the chitosan/marble powder composites, 0.1 g adsorbent was added into 50 mL Dimozol Blue solution with fixed concentrations (60 mg L^{-1}). The mixtures were kept in a thermostat shaker (Termal H11960) with a shaking speed of 150 rpm at natural pH and room temperature for 72 h. At a predetermined time period, an aqueous sample (5 mL) was taken from the solution, and the concentrations of dye solution were determined using UV–vis spectroscopy (Agilent Cary 60 UV-Vis) at a wavelength of 610 nm. The amount adsorbed on the chitosan/marble powder composites at any time was calculated by the following equation (Crini & Badot 2008):

$$q_t = \frac{(C_0 - C_t)V}{m} \quad (1)$$

where C_0 (mg L^{-1}) is the initial dye concentration; C_t (mg L^{-1}) is the dye concentration at time t (h); V (L) is the volume of the solution, and m (g) is the mass of the adsorbent.

RESULTS AND DISCUSSION

Characterization

SEM images of the cross-linked chitosan/marble powder composites envisioned at magnifications of $74 \times (100\ \mu m)$ and $520 \times (20\ \mu m)$ are shown in Figures 1 and 2. From the SEM micrograph in Figure 1, it is observed that the all composites exhibit a porous texture.

As shown in Figure 2, the composites with lesser amounts of marble powder have a smooth surface.

In the adsorption process, the surface area of the adsorbents is the most important factor. In the BET analysis, the effects of marble powder and chitosan contents on the surface areas of the adsorbents were detected. As shown in

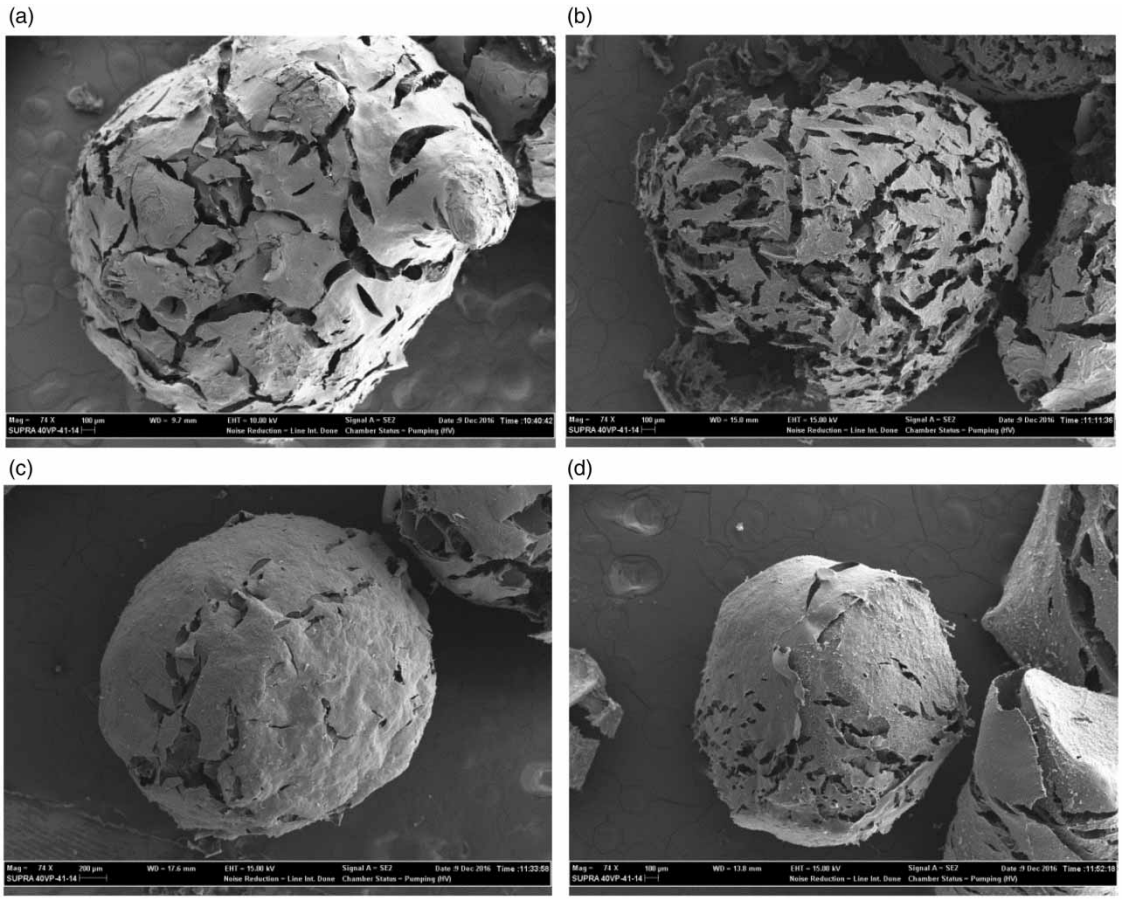

Figure 1 | SEM images of C100M0 (a), C70M30 (b), C50M50 (c), and C30M70 (d).

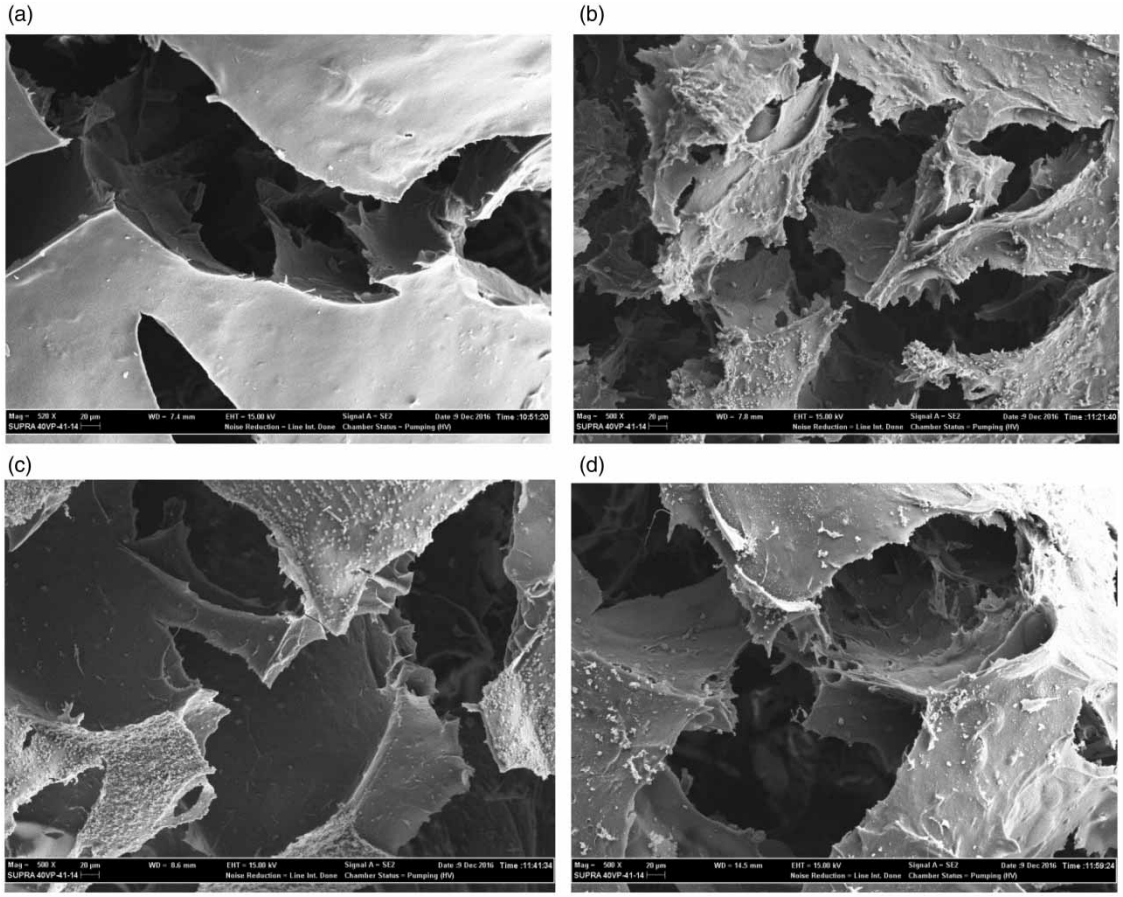

Figure 2 | SEM images of the pore structure of the porous C100M0 (a), C70M30 (b), C50M50 (c), and C30M70 (d).

Table 1, the surface area of the adsorbent increases from 17.9 m^2/g to 34.3 m^2/g as the amounts of marble powder in the adsorbent matrix are increased from 0 to 30 wt. %. An additional increase in the marble powders indicates a decline in the surface of C50M50 and C30M70 (i.e. 23.1 $m^2\,g^{-1}$ and 0.2 $m^2\,g^{-1}$, respectively). The sharp decrease in surface area of the composites is considered to be due to an increase in agglomeration of the marble powders on the top layer and inside the channel of the adsorbent matrix (Gebru & Das 2017).

Table 1 | Effects of marble powder and chitosan contents on adsorbent surface area

Adsorbent	Chitosan content (wt. %)	Marble powder content (wt. %)	Specific surface area (m^2/g)
C100M0	100	0	17.9
C70M30	70	30	34.3
C50M50	50	50	23.1
C30M70	30	70	0.2

The EDS characterization was used to analyze the elemental composition of the composites. As can be seen in Figure 3, C and O elements are detected in all composites, whereas Ca element is only detected in C70M30, C50M50, and C30M70 composites due to the marble powder content of the composites.

In order to study the functional groups' content in the chitosan/marble powder composites, the composites were characterized using FTIR. The FTIR spectrum of the composites were compared with FTIR spectrum of chitosan and marble powder. The comparison of these spectra was shown in Figure 4. Figure 4(b) shows the FTIR spectrum of chitosan. It confirmed the presence of saturated hydrocarbons in the structure of chitosan. Stretching vibrations of NH_2 occurred at wave number 3,489 cm^{-1}. Stretching vibrations of –OH appeared at wave number 3,213 cm^{-1}. FTIR spectra of marble powder display characteristic absorption bands in the region 1,850–650 cm^{-1} corresponding to C–O bond vibrations. FTIR spectrum of the chitosan/marble powder composites (Figure 4(a)) shows the combination of

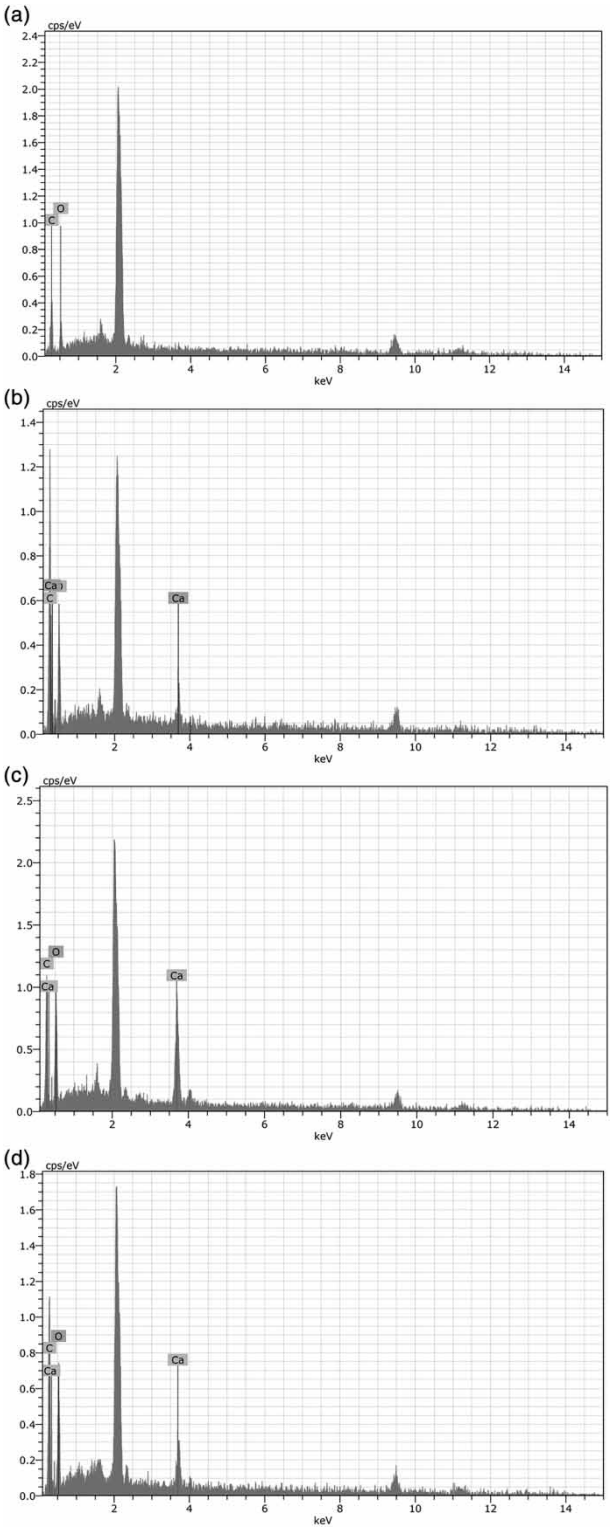

Figure 3 | EDS patterns of C100M0 (a), C70M30 (b), C50M50 (c), and C30M70 (d).

chitosan and marble powder. The wavenumbers of functional groups in the structure of chitosan and marble powder also appeared in the composites (Marrakchi *et al.* 2016).

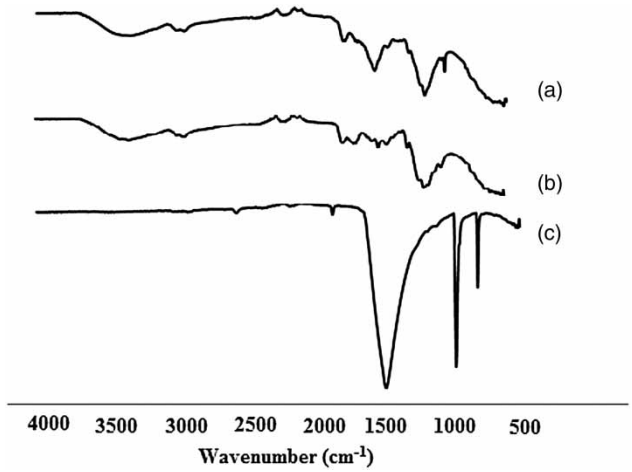

Figure 4 | FTIR spectra of (a) chitosan/marble powder composites, (b) chitosan, and (c) marble powder.

Effects of contact time in the adsorption process

Contact time is an important variable in adsorption processes. In the literature, most studies about chitosan-based adsorbents show that the adsorption of dyes is fast in the initial stages of the treatment time due to the availability of a large number of vacant surface sites. Thereafter, the adsorption process becomes slower near the equilibrium because of difficulty in occupying the remaining vacant surface sites due to the repulsive forces between dye molecules adsorbed on the adsorbent surface and those in the solution phase. Thus, the contact time for equilibrium to be attained is in the range of 3–5 days for most dye molecules (Crini & Badot 2008).

The effects of contact time on the adsorption uptake of different chitosan/marble powder composites (C100M0, C70M30, C50M50, and C30M70) for Dimozol Blue were examined at various time intervals, and the results obtained are presented in Figure 5. It was observed that the adsorption capacity increased with increasing contact time and reached equilibrium after 72 h. The adsorption amount of Dimozol Blue dye onto the adsorbents at various time intervals followed the order of C70M30 > C50M50 > C100M0 > C30M70. At equilibrium, the adsorption capacity of Dimozol Blue onto C100M0, C70M30, and C50M50 was about 27 mg/g and higher than that onto C30M70. C50M50 composites were more economical than C100M0 and C70M30 due to the higher marble powder content and hence were selected as an adsorbent for all the other studies.

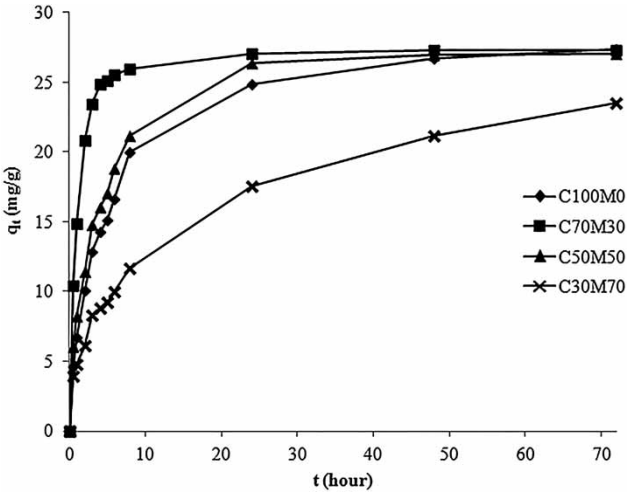

Figure 5 | Effect of contact time on the adsorption of Dimozol Blue onto chitosan/marble powder composites (adsorption conditions: adsorbent dosage 2 g/L; initial concentration of dye 60 mg/L; solution volume 50 mL; agitation speed 150 rpm; medium pH 6; temperature 25 °C).

Adsorption kinetic models

Two kinetic models, the pseudo-first-order and pseudo-second-order kinetic models, were used to examine the adsorption mechanism. The pseudo-first-order and pseudo-second-order are defined as in the following two equations, respectively (Lagergren 1898; Ho & McKay 1999):

$$\log(q_e - q_t) = \log q_e - \frac{k_1}{2.303}t \quad (2)$$

$$\frac{t}{q_t} = \frac{1}{k_2 q_e^2} + \frac{t}{q_e} \quad (3)$$

where k_1 and k_2 are the pseudo-first-order and pseudo-second-order rate constant, respectively; and q_t and q_e are the adsorption capacity of Dimozol Blue dye at time t and at equilibrium, respectively.

The parameters of kinetic models and correlation coefficients (R^2) for Dimozol Blue dye adsorption on different chitosan/marble powder composites are depicted in Table 2. It is obvious that the corresponding linear regression correlation coefficient (R^2) value for the pseudo-second-order model is relatively higher than that for the pseudo-first-order. Moreover, the calculated q_e values obtained from the pseudo-second-order kinetic model agree with the experimental data ($q_{e,exp}$) better than the ones obtained from pseudo-first-order. It is demonstrated that the adsorption of the Dimozol Blue dye onto the chitosan/marble powder composites can be described by the pseudo-second-order kinetic much better than the pseudo-first-order model.

Effect of pH

The pH of the solution affects the surface charge of the adsorbents as well as the degree of ionization of dye molecules. The effect of the pH of Dimozol Blue solution on the adsorption capacity of C50M50 was investigated in the pH range 3–11 (Figure 6). The initial pH ranged from 11 to 5, the adsorption capacity of Dimozol Blue onto the C50M50 composites increased with pH until the pH reached 5, and then the adsorption capacities slightly decreased with a further decrease in the pH value. The highest amounts of adsorbed Dimozol Blue were observed at pH 5. At pH values lower than 5, the adsorbents may dissolve, thereby it may cause a decrease in the number of available adsorption sites on the chitosan/marble powder composites, leading to a lower adsorption capacity.

Effect of adsorbent dosage

The effect of adsorbent dosage was investigated by the batch equilibrium technique using 50 mL dye solution by varying the adsorbent mass (0.010, 0.025, 0.050, and 0.100 g), and the results of this study are graphed in Figure 7. The adsorbed amount decreased from 155.6 mg/g to 28.0 mg/g when the adsorbent dosage was increased from 0.01 g to 0.1 g. The decrease of adsorption was due to the concentration gradient between adsorbent and adsorptive.

Table 2 | Kinetic parameters for Dimozol Blue dye adsorption on different chitosan/marble powder composites

	Pseudo-first-order				Pseudo-second-order		
Adsorbents	$q_{e,exp}$ (mg/g)	$q_{e,cal}$ (mg/g)	k_1 ($\times 10^3$) (hour^{-1})	R^2	$q_{e,cal}$ (mg/g)	k_2 ($\times 10^3$) (hour^{-1})	R^2
C100M0	27.36	19.26	75.3	0.9640	28.49	10.8	0.9975
C70M30	27.33	9.27	172.7	0.9436	27.55	70.3	0.9999
C50M50	27.01	19.92	133.3	0.9930	28.01	15.6	0.9984
C30M70	23.48	18.73	45.1	0.9787	24.45	40.9	0.9836

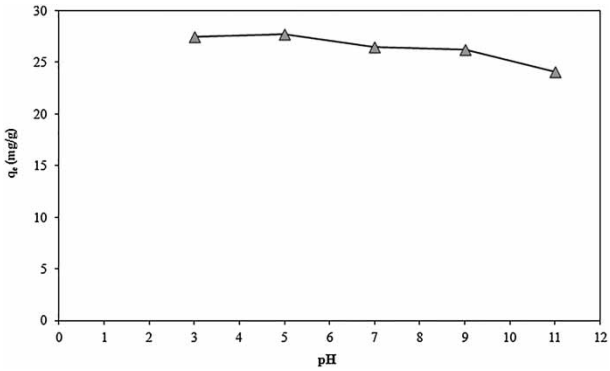

Figure 6 | Effect of pH on the adsorption capacity of C50M50 composites (adsorption conditions: adsorbent dosage 2 g/L; initial concentration of dye 60 mg/L; solution volume 50 mL; agitation speed 150 rpm; temperature 25 °C; contact time 72 h).

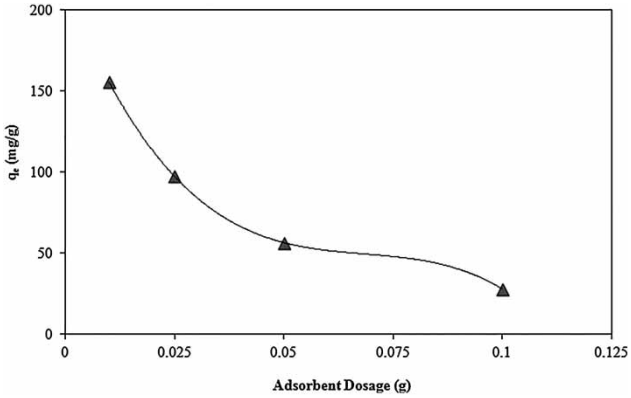

Figure 7 | Effect of adsorbent dosage on the adsorption capacity of C50M50 composites (adsorption conditions: initial concentration of dye 60 mg/L; solution volume 50 mL; agitation speed 150 rpm; medium pH 6; temperature 25 °C; contact time 72 h).

Adsorption isotherm models

Four different concentrations (40, 60, 80 and 100 mg/L) were selected to investigate the effect of initial dye concentration on the adsorption of Dimozol Blue dye onto the C50M50 composites. Figure 8 shows the adsorption isotherm for Dimozol Blue adsorption on the C50M50 composites. It reveals that the amount of dye adsorbed increased from 111.3 mg/g to 234.5 mg/g when the initial dye concentration was increased from 40 mg/L to 100 mg/L.

The adsorption isotherm models were applied to understand the interaction between adsorbate and adsorbent, whether it was a single layer (Langmuir) or a multilayer (Freundlich) adsorption. The linear forms of Freundlich and Langmuir isotherm models are shown in Equations (4) and (5), respectively (Crini & Badot 2008).

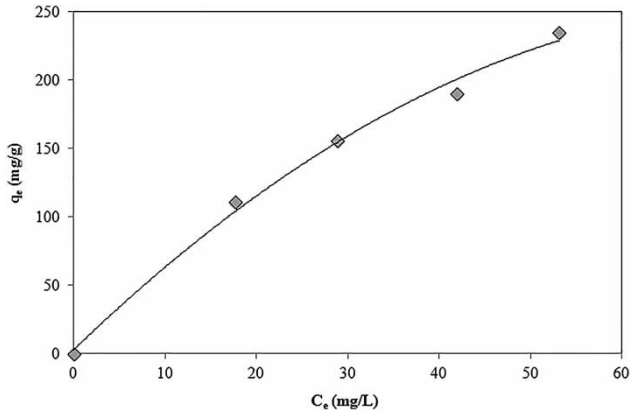

Figure 8 | Equilibrium adsorption isotherm of Dimozol Blue onto the C50M50 composites (adsorption conditions: initial concentration of dye 40–100 mg/L adsorbent dosage 0.2 g/L; solution volume 50 mL; agitation speed 150 rpm; medium pH 6; temperature 25 °C; contact time 72 h).

$$\ln q_e = \ln K_F + \left(\frac{1}{n}\right) . (\ln C_e) \quad (4)$$

$$\frac{C_e}{q_e} = \frac{C_e}{q_m} + \frac{1}{(q_m . K_L)} \quad (5)$$

where C_e (mg/L) represents the equilibrium concentration of Dimozol Blue, C_0 (mg/L) is the initial concentration of Dimozol Blue, q_e (mg/g) is the amount of Dimozol Blue adsorbed per gram of adsorbent, q_m is the maximum adsorption capacity (mg/g), and K_L is a Langmuir constant (L/g) related to the affinity towards the binding sites and energy of adsorption. K_F and n are the Freundlich constants, which measure the adsorption capacity and intensity, respectively.

Adsorption parameters obtained from the Freundlich and Langmuir isotherm models are given in Table 3. The Langmuir isotherm model assumes monolayer coverage of adsorbates onto adsorbents and uniform energies of adsorption on the surface of adsorbent. The correlation coefficient result for the Langmuir isotherm (0.9487) is not a satisfactorily good correlation between the model prediction and the experimental data. The results showed that the Freundlich model, with the higher value of correlation coefficient ($R^2 = 0.9943$) fitted better than the Langmuir isotherm

Table 3 | Adsorption isotherm constants for Dimozol Blue adsorption onto the C50M50 composites

Freundlich			Langmuir		
K_F [mg/g (L/g)$^{1/n}$]	n	R^2	q_m (mg/g)	K_L (L/mg)	R^2
16.6448	1.5135	0.9943	500.0	0.0157	0.9487

model. The Freundlich isotherm model assumes the adsorption process occurs as multilayer coverage on the heterogeneous surface of the adsorbent due to the diversity of adsorption sites (Tadjarodi *et al.* 2016). Moreover, the value of n is greater than 1, indicating that the adsorption process is favorable.

Adsorption thermodynamics

The effect of temperature on the adsorption isotherm was investigated under isothermal conditions in the temperature range of 298–318 K. The adsorption capacity decreased with the increase in temperature.

Thermodynamic parameters such as change in free energy (ΔG°) (kJ/mol), enthalpy (ΔH°) (kJ/mol), and entropy (ΔS°) (J/mol·K) were calculated by using the following thermodynamic equations (Crini & Badot 2008):

$$\ln K_C = \frac{\Delta S^\circ}{R} - \frac{\Delta H^\circ}{RT} \quad (6)$$

$$K_C = \frac{q_e}{C_e} \quad (7)$$

$$\Delta G^\circ = \Delta H^\circ - T\Delta S^\circ \quad (8)$$

where R is the universal gas constant (8.314 J/mol·K). T and K_c are the absolute temperature (K) and thermodynamic equilibrium constant, respectively. The values of ΔS° and ΔH° were obtained from the intercept and slope of the plot ln K_c (q_e/C_e) vs 1/T, these values are shown in Table 4.

The negative values of ΔG° confirm the feasibility of the process and the spontaneous nature of the adsorption of Dimozol Blue molecules onto the C50M50 composites. ΔG is more negative with decreasing temperature from 318 K to 298 K, which suggests that lower temperature makes the adsorption easier. The negative (−37.4 kJ/mol) for Dimozol Blue adsorption is an exothermic process in accordance with the decreasing adsorption capacity with increasing temperature. Generally, ΔH for physical adsorption ranges from −4 to −40 kJ/mol, compared to that of chemical adsorption ranging from −40 to −800 kJ/mol (Crini & Badot 2008). Therefore based on the ΔH° value, the adsorption of Dimozol Blue onto the C50M50 composite surface is physical adsorption. In addition, the negative value of ΔS° (−89.2 J/mol K) suggests that the randomness decreased at the solid/solution interface as a results of Dimozol Blue adsorption onto the C50M50 composite surface.

Table 4 | Thermodynamic parameters for Dimozol Blue dye adsorption onto the C50M50 composites

T (K)	ΔH° (kJ/mol)	ΔS° (J/mol·K)	ΔG° (kJ/mol)
298			−10.82
308	− 37.4	− 89.2	−9.93
318			−9.03

Table 5 | Comparison of the maximum adsorption capacities of the different adsorbents for the removal of Reactive Blue 221 dye

Adsorbent	Maximum adsorption capacity (mg/g)	BET surface area (m^2/g)	References
Calcinated sepiolite	27.1–32.5	357	Alkan *et al.* (2005)
Kaolinite	12.4	17	Karaoğlu *et al.* (2010)
Pumice stone	54.20	8.47	Aksu *et al.* (2011)
Cross-linked chitosan/marble powder composites, C50M50	234.5	23.1	This work

For comparison, the different adsorbents for adsorption of Reactive Blue 221 dye are listed in Table 5. The adsorption capacity of the cross-linked chitosan/marble powder composites in this work is considerably higher than that of others reported in the literature.

CONCLUSIONS

In this study, the chitosan/marble powder composites with different weight ratio percentage (C100M0, C70M30, C50M50 and C30M70) were synthesized and used as adsorbents for Dimozol Blue dye. The experimental results indicated that chitosan/marble powder composites, especially C100M0, C70M30 and C50M50, were effective adsorbents for the removal of Dimozol Blue dye from aqueous solution. The adsorption experimental data agreed perfectly with the pseudo-second-order kinetic equation, where the regression coefficients were greater than 98% ($R^2 > 0.98$) for all composites. The results showed that the adsorption was also influenced by factors including contact time, pH value, adsorbent dosage, initial concentration of dye, and temperature. Under the optimal conditions (contact time: 72 hours; pH:5; initial dye concentration: 100 mg/L; adsorbent dosage: 0.01 g; 25 °C), the experimental maximum adsorption capacity achieved was 234.5 mg/g.

The attractive features of marble powder and chitosan make the composites effective, economic, and environmentally friendly adsorbents.

REFERENCES

Aksu, A., Murathan, A. & Kocyigit, H. 2011 Adsorption of reactive blue 221 on pumice stone and kinetic study. *Journal of the Faculty of Engineering and Architecture of Gazi University* **26** (4), 807–812.

Alkan, M., Çelikçapa, S., Demirbaş, Ö. & Doğan, M. 2005 Removal of reactive blue 221 and acid blue 62 anionic dyes from aqueous solutions by sepiolite. *Dyes and Pigments* **65** (3), 251–259.

Alyamac, K. E., Ghafari, E. & Ince, R. 2017 Development of eco-efficient self-compacting concrete with waste marble powder using the response surface method. *Journal of Cleaner Production* **144**, 192–202.

Arica, T. A., Ayas, E. & Arica, M. Y. 2017 Magnetic MCM-41 silica particles grafted with poly(glycidylmethacrylate) brush: Modification and application for removal of direct dyes. *Microporous and Mesoporous Materials* **243**, 164–175.

Auta, M. & Hameed, B. H. 2014 Chitosan–clay composite as highly effective and low-cost adsorbent for batch and fixed-bed adsorption of methylene blue. *Chemical Engineering Journal* **237**, 352–361.

Bayramoglu, G., Altintas, B. & Arica, M. Y. 2009 Adsorption kinetics and thermodynamic parameters of cationic dyes from aqueous solutions by using a new strong cation-exchange resin. *Chemical Engineering Journal* **152** (2), 339–346.

Bayramoglu, G., Adiguzel, N., Ersoy, G., Yilmaz, M. & Arica, M. Y. 2013 Removal of textile dyes from aqueous solution using amine-modified plant biomass of A. caricum: equilibrium and kinetic studies. *Water, Air & Soil Pollution* **224** (8), 1640.

Crini, G. & Badot, P. M. 2008 Application of chitosan, a natural aminopolysaccharide, for dye removal from aqueous solutions by adsorption processes using batch studies: a review of recent literature. *Progress in Polymer Science* **33** (4), 399–447.

Dinu, M. V. & Dragan, E. S. 2010 Evaluation of Cu^{2+}, Co^{2+} and Ni^{2+} ions removal from aqueous solution using a novel chitosan/clinoptilolite composite: kinetics and isotherms. *Chemical Engineering Journal* **160** (1), 157–163.

Dotto, G. L., Rodrigues, F. K., Tanabe, E. H., Fröhlich, R., Bertuol, D. A., Martins, T. R. & Foletto, E. L. 2016 Development of chitosan/bentonite hybrid composite to remove hazardous anionic and cationic dyes from colored effluents. *Journal of Environmental Chemical Engineering* **4** (3), 3230–3239.

Gebru, K. A. & Das, C. 2017 Removal of Pb (II) and Cu (II) ions from wastewater using composite electrospun cellulose acetate/titanium oxide (TiO_2) adsorbent. *Journal of Water Process Engineering* **16**, 1–13.

Ho, Y. S. & McKay, G. 1999 Pseudo-second order model for sorption processes. *Process Biochemistry* **34** (5), 451–465.

Jóźwiak, T., Filipkowska, U., Szymczyk, P., Rodziewicz, J. & Mielcarek, A. 2017 Effect of ionic and covalent crosslinking agents on properties of chitosan beads and sorption effectiveness of Reactive Black 5 dye. *Reactive and Functional Polymers* **114**, 58–74.

Karaoğlu, M. H., Doğan, M. & Alkan, M. 2010 Kinetic analysis of reactive blue 221 adsorption on kaolinite. *Desalination* **256** (1), 154–165.

Khan, S. A., Khan, S. B., Kamal, T., Yasir, M. & Asiri, A. M. 2016 Antibacterial nanocomposites based on chitosan/Co-MCM as a selective and efficient adsorbent for organic dyes. *International Journal of Biological Macromolecules* **91**, 744–751.

Lagergren, S. 1898 Zur theorie der sogenannten adsorption geloster stoffe. *Kungliga Svenska Vetenskapsakademiens Handlingar* **24**, 1–39.

Marrakchi, F., Khanday, W. A., Asif, M. & Hameed, B. H. 2016 Cross-linked chitosan/sepiolite composite for the adsorption of methylene blue and reactive orange 16. *International Journal of Biological Macromolecules* **93**, 1231–1239.

Nesic, A. R., Velickovic, S. J. & Antonovic, D. G. 2012 Characterization of chitosan/montmorillonite membranes as adsorbents for Bezactiv Orange V-3R dye. *Journal of Hazardous Materials* **209**, 256–263.

Silva, T. L., Ronix, A., Pezoti, O., Souza, L. S., Leandro, P. K., Bedin, K. C., Beltrame, K. K., Cazetta, A. L. & Almeida, V. C. 2016 Mesoporous activated carbon from industrial laundry sewage sludge: adsorption studies of reactive dye Remazol Brilliant Blue R. *Chemical Engineering Journal* **303**, 467–476.

Singh, H., Chauhan, G., Jain, A. K. & Sharma, S. K. 2017 Adsorptive potential of agricultural wastes for removal of dyes from aqueous solutions. *Journal of Environmental Chemical Engineering* **5** (1), 122–135.

Su, C. X. H., Low, L. W., Teng, T. T. & Wong, Y. S. 2016 Combination and hybridisation of treatments in dye wastewater treatment: a review. *Journal of Environmental Chemical Engineering* **4** (3), 3618–3631.

Tadjarodi, A., Ferdowsi, S. M., Zare-Dorabei, R. & Barzin, A. 2016 Highly efficient ultrasonic-assisted removal of Hg(II) ions on graphene oxide modified with 2-pyridinecarboxaldehyde thiosemicarbazone: adsorption isotherms and kinetics studies. *Ultrasonics Sonochemistry* **33**, 118–128.

Yavuz, E., Bayramoğlu, G., Arica, M. Y. & Senkal, B. F. 2011 Preparation of poly(acrylic acid) containing core-shell type resin for removal of basic dyes. *Journal of Chemical Technology and Biotechnology* **86** (5), 699–705.

Yuliani, G., Garnier, G. & Chaffee, A. L. 2017 Utilization of raw and dried Victorian brown coal in the adsorption of model dyes from solution. *Journal of Water Process Engineering* **15**, 43–48.

Zhang, L., Hu, P., Wang, J. & Huang, R. 2016 Adsorption of Amido Black 10 B from aqueous solutions onto Zr(IV) surface-immobilized cross-linked chitosan/bentonite composite. *Applied Surface Science* **369**, 558–566.

First received 10 May 2017; accepted in revised form 24 July 2017. Available online 3 August 2017